Chemistry & Biology, Vol. 9, 375–381, March, 2002, ©2002 Elsevier Science Ltd. All rights reserved. PII S1074-5521(02)00112-6

MgF_3^- as a Transition State Analog of Phosphoryl Transfer

Debbie L. Graham,[1] Peter N. Lowe,[1] Geoffrey W. Grime,[2] Michael Marsh,[2] Katrin Rittinger,[3] Stephen J. Smerdon,[3] Steven J. Gamblin,[3,4] and John F. Eccleston[3]

[1]Computational & Structural Sciences
GlaxoSmithKline
Gunnels Wood Road
Stevenage, Herts
United Kingdom

[2]SPM Unit
Nuclear Physics Laboratory
University of Oxford
United Kingdom

[3]National Institute for Medical Research
Mill Hill, London NW7 1AA
United Kingdom

Summary

The formation of complexes between small G proteins and certain of their effectors can be facilitated by aluminum fluorides. Solution studies suggest that magnesium may be able to replace aluminum in such complexes. We have determined the crystal structure of RhoA.GDP bound to RhoGAP in the presence of Mg^{2+} and F^- but without Al^{3+}. The metallofluoride adopts a trigonal planar arrangement instead of the square planar structure of AlF_4^-. We have confirmed that these crystals contain magnesium and not aluminum by proton-induced X-ray emission spectroscopy. The structure adopted by GDP.MgF^- possesses the stereochemistry and approximate charge expected for the transition state. We suggest that MgF3$^-$ may be the reagent of choice for studying phosphoryl transfer reactions.

Introduction

In biological systems, the transfer of high-energy phosphate groups is the principal means of storing and transferring chemical energy as well as being a key mechanism of cellular signaling and regulation. As such, the enzymology of phosphoryl transfer has been the subject of intense study for many years. Since the first report that aluminum is a necessary factor in the fluoride-dependent activation of heterotrimeric G proteins [1], it has become an essential tool in the study of phosphoryl-transferring enzymes such as GTPases, ATPases, and kinases. In the presence of a nucleoside di-phosphate (NDP), alumino-fluorides (AlF_x) bind to these enzymes at a site that would otherwise accommodate the γ-phosphate group of NTP's.

The chemical nature of the AlF_x species which bind to phosphoryl-transferring proteins is complex because, in aqueous solution, they form a mixture of chemical species that depends on fluoride concentration and pH [2], [3]. It was originally assumed that a tetrahedral complex of AlF_4^- acted as a mimic of the γ-phosphate of GTP thus converting the GDP bound form of transducin to the active GTP-like form [4].

Many different crystal structures of protein/nucleotide complexes containing AlF_x have now been reported. For all the cases involving small G proteins, the arrangement of GDP.AlF_x.H_2O has been interpreted as mimicking the transition state of the phosphoryl transfer reaction. The hydrolysis of GTP proceeds by an in-line nucleophilic attack by a water molecule on the γ-phosphate leading to inversion of the configuration of stereochemistry. The transition state involves the γ-phosphate adopting a trigonal bipyramidal arrangement with the axial coordination sites being occupied by oxygens from the β-phosphate and hydrolytic water molecule. Although unproven, there is a general expectation that GTPase catalyzed GTP hydrolysis proceeds through a transition state that is largely dissociative in character [5].

The structures of NDP kinase [6], UMP kinase [7], Ras.RasGAP [8], and Cdc42.RhoGAP [9] each contain AlF_3^-. The penta-coordinated aluminum ion interacts with three equatorial fluorides, while the two axial positions are occupied by an oxygen atom from the β-phosphate of the nucleoside di-phosphate and another oxygen from the attacking nucleophile. This trigonal bipyramidyl geometry is that expected for the phosphoryl group during the transition state of the reaction. In contrast, structures of transducin [10], G_{ia} [11], myosin subfragment 1 [12], and Rho.RhoGAP [13] contain an octahedrally coordinated aluminum ion. In this case, the metallo-fluoride carries a net negative charge as would be expected for this moiety of the transition state species, but the four fluorides adopt a square planar arrangement.

There have been reports that heterotrimeric G proteins can be activated by fluoride, apparently in the absence of aluminum. Gilman and his colleagues have shown that Mg^{2+} is capable of mimicking the effect of Al^{3+} at very high concentrations of fluoride [14]. This work was later extended and a model was proposed in which Mg^{2+} associates with three fluorides and mimics the γ-phosphate of GTP [15]. More recently it has been shown qualitatively that Rho.GDP can form a tight complex with p190 RhoGAP in the presence of fluoride but absence of aluminum [16]. A more quantitative characterization of this phenomenon has recently been carried out that shows that RhoA is able to bind to RhoGAP in a magnesium fluoride-dependent manner with apparent affinities of 0.48 μM and 0.28 μM in the presence and absence of aluminum, respectively [17]. We now demonstrate, by crystallographic and spectroscopic analysis, that magnesium is, indeed, able to substitute for aluminum in these complexes and that GDP.MgF_3^- forms a transition state (rather than a GTP-like ground state) analog with the appropriate charge and geometry for the phosphoryl transfer reaction catalyzed by small GTPases.

[4]Correspondence: sgambli@nimr.mrc.ac.uk

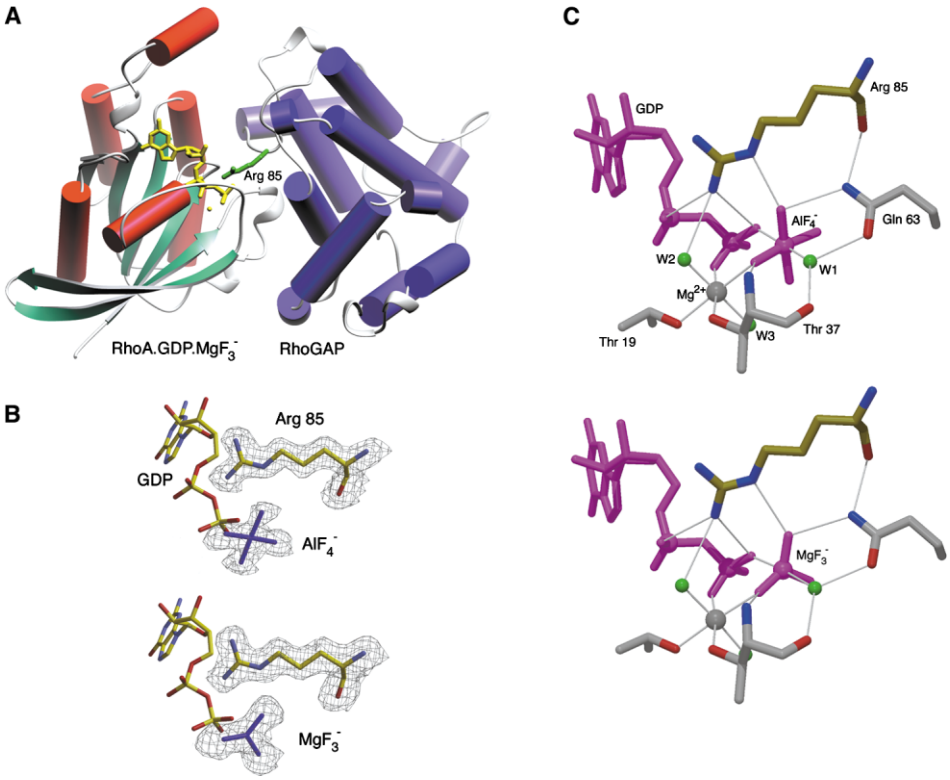

Figure 1. Crystal Structures of Rho/RhoGAP Complex

(A) shows the complex between the catalytic GAP domain of p50RhoGAP (α helices shown as blue cylinders) and the Mg.GDP.MgF_3^- (shown as yellow ball and stick) complex of RhoA (α helices as red cylinders and β strands in green). The catalytic arginine residue (R85) from the GAP domain is shown in green interacting with the metallo-fluoride moiety. The overall arrangements of the two proteins and the interactions made at their interface are very similar to those previously described for the complex of RhoA.Mg.GDP.AlF_4^-/RhoGAP [13]. The figure was produced with the program Ribbons [29].

(B) The top and bottom panels show electron density maps for the "AlF_4^-" and "MgF_3^-" complexes, respectively, together with a ball-and-stick representation for the catalytic R85 from RhoGAP, the GDP, and the metallo-fluoride moiety. The electron density maps were calculated with (Fo − Fc) coefficients where the amplitudes and phases were calculated from the atomic model with the coordinates for R85 and the metallo-fluoride omitted from the last cycles of refinement.

(C) The top panel shows, in ball-and-stick representation, molecular details of the active site of the complex with "AlF_4^-" while the bottom panels show the same view for the complex with "MgF_3^-." Arg 85 from RhoGAP is colored yellow while the residues from RhoA are shown in gray. The GDP and metallo-fluoride moiety are shown in magenta while water molecules are in green. The distances for the various interactions shown are presented in Table 3. The interactions of Lys18 and Gly62 of Rho with the metallo-fluoride moiety have been omitted from this figure (but not 2B and 2C) for clarity.

Results

Crystallographic Analysis

We have previously probed the structural and mechanistic basis of GTPase-activating protein (GAP) function by determining the structure of the catalytic domain of p50RhoGAP and its complexes with Cdc42Hs.GMPPNP [18] and RhoA.GDP.AlF_4^- [13]. The latter two complexes have been described as representing ground-state and transition-state mimics of the nucleotide, respectively. To address the fluoride-dependent role of aluminum and magnesium in mimicking the transition state of phosphoryl transfer reactions, we have grown crystals of RhoA.GDP/p50RhoGAP in the presence of 10 mM magnesium but in the absence of aluminum. To ensure that there was no contamination with aluminum, all crystallization work was carried out in the presence of the powerful aluminum chelator deferoxamine [19].

The structure of the "magnesium" crystal form was solved by molecular replacement using separate models for the G protein and the RhoGAP. The crystal structure shows that the two proteins adopt the same relative orientation as in the AlF_4^- complex (Figure 1A). Moreover, given the relatively high-resolution diffraction limit of both the present structure (1.8 Å) and the previously reported RhoA.GDP.AlF_4^-/p50RhoGAP complex (1.65 Å), we are confident that the details of the protein-protein interface are essentially unchanged.

Automated model refinement produced a high quality Fourier map with clear electron density for the metallo-fluoride moiety without it being explicitly included in the atomic model (Table 1). A portion of the electron density map covering this region is shown in Figure 1B together with relevant parts of the atomic model, while a detailed view of the active site for both the AlF_4^- and MgF_3^- complex is shown in Figure 1C. The experimental data suggest that there is a metal ion coordinated by three equatorial fluoride ligands and by a β-phosphate oxygen

Table 1. Crystallographic Statistics for Rho.GDP.MgF_3^-/RhoGAP Crystal

Data	
Resolution limits (Å)	15.0 to 1.8
Space group $P2_12_12_1$, unit cell (Å)	a = 66.5, b = 71.4, c = 91.5
% completeness	99.6 (99.9)
Number of total observations	218,823
Number of unique observations	40,618
R_{sym} (%)	8.3 (40.1)
Wilson B factor (Å^2)	20
Refinement	
R_{cryst}	18.3 (20.5)
R_{free}	22.0 (24.4)
Rms bonds (Å)	0.007
Rms angles (°)	1.5
Number of waters	390

Values in parentheses apply to the highest resolution bin.

and the hydrolytic water molecule in the apical positions (Figure 1C). Although there are differences in bond lengths and angles made by the AlF_4^- and MgF_3^- moieties with the protein, there is only one interaction that involves different atoms in the two cases. The side chain of Lysine 18 and the main chain amide of Glycine 62 from RhoA both interact with F1 of the MgF_3^- moiety whereas the interactions are shared between F1 and F4 in the AlF_4^- case (Figures 2B and 2C).

Proton-Induced X-Ray Emission analysis

The X-ray scattering properties of aluminum and magnesium are not sufficiently different to allow them to be distinguished by X-ray crystal diffraction data. Although there should be no free aluminum in the crystallization buffer, we determined the metal content of the crystals directly by proton-induced X-ray emission (PIXE) on the Oxford scanning proton microprobe facility. PIXE [20], [21], [22] gives minimum detectable limits in the range of 1–100 parts per million by weight for all elements with $Z > 11$ in the periodic table. For comparison, we carried out the same measurements on the original crystal form containing RhoA.GDP.AlF_4^-/RhoGAP. To provide an internal calibration for the amount of magnesium and aluminum present in the two different crystal forms we also measured the amount of phosphorus present. Phosphorus was chosen because, in both crystal forms, there are just two phosphate groups present in each protein/protein complex due to the GDP. If a high abundance atom, for example carbon, was used as an internal reference, the ratio of magnesium or aluminum to carbon could not be accurately determined. The use of an internal calibration means that the amounts of aluminum and magnesium can be expressed as a simple ratio (with respect to phosphorus content) and means that accurate quantitative measurements are possible without knowing the normalization factor required to express the true concentration on an absolute scale.

If the metallo-fluoride moiety at the active site is MgF_3^-, then each small G protein complex in the crystal should contain two phosphorus atoms and two magnesium ions, one magnesium ordinarily being associated with the GDP (or GTP) bound to the G protein. The PIXE analysis showed that the new crystals contained magnesium and phosphorus in the ratio 0.86 ($\pm$0.1) and that there was no detectable aluminum present (Table 2). These data are in close agreement to the expected magnesium/phosphorus ratio of 1.0. Taken together with the absence of aluminum from the crystals, this data strongly supports the notion that it is indeed MgF_3^- that is present at the active site.

In contrast, the original RhoA.GDP.AlF_4^-/RhoGAP crystals should contain two phosphorus atoms, one aluminum atom, and just one magnesium atom. The PIXE analysis of these crystals showed aluminum and magnesium present in the ratio 0.9 ($\pm$0.16) and the ratio of magnesium to phosphorus and aluminum to phosphorus to be 0.34 ($\pm$0.04) and 0.39 ($\pm$0.05), respectively. These results are reasonably close to the expected ratios of 1.0, 0.5, and 0.5. These data establish that the PIXE procedure can detect very small amounts of aluminum from crystal samples. This in turn gives further confidence that the PIXE results from the "magnesium" crystal are reliable in establishing that they do not contain aluminum.

Discussion

The PIXE analysis presented here provides a reliable and direct demonstration that MgF_3^- is able to substitute for AlF_4^- at the active site of RhoA.GDP/RhoGAP. This is important for several reasons. Although the quality of the X-ray structure determination presented here is very good, it cannot distinguish between two metals of such similar atomic numbers as aluminum ($Z = 13$) and magnesium ($Z = 12$). Importantly, the PIXE analysis shows both that the "magnesium" crystals do contain magnesium, and that they do not contain aluminum. The data from the "aluminum" crystals confirm that they contain equal amounts of aluminum and magnesium, thus providing the necessary control that the PIXE procedure is able to detect the single aluminum ions present in each RhoA/RhoGAP complex in the crystal.

The structural analysis of RhoA.GDP/RhoGAP crystallized in the presence of Mg^{2+} and F^- provides a structural description of magnesium fluoride acting as part of a transition state analog. The relatively high-resolution limit of the diffraction data (1.8 Å) yields a very well-defined electron density map, revealing that MgF_3^- coordinates with one oxygen of the β-phosphate of GDP and another from the hydrolytic water molecule, in a trigonal bipyramidal arrangement. This organization of ligands around the metal is unusual because magnesium often adopts six coordination geometry. Nevertheless, examples have been described of magnesium adopting penta-covalent bonding with distorted trigonal bipyramidal geometry [23].

It is interesting to compare the structure and activity of MgF_3^- with that of another metallo-trifluoride used in the study of enzymatic phosphoryl transfer systems, namely BeF_3^-. Although both metals are coordinated by three fluorides, and each moiety carries a net negative charge, the geometry and activity of these two compounds is quite different. BeF_3^- adopts a tetrahedral arrangement in contrast to the trigonal planar geometry of MgF_3^-. This difference in coordination is presumably

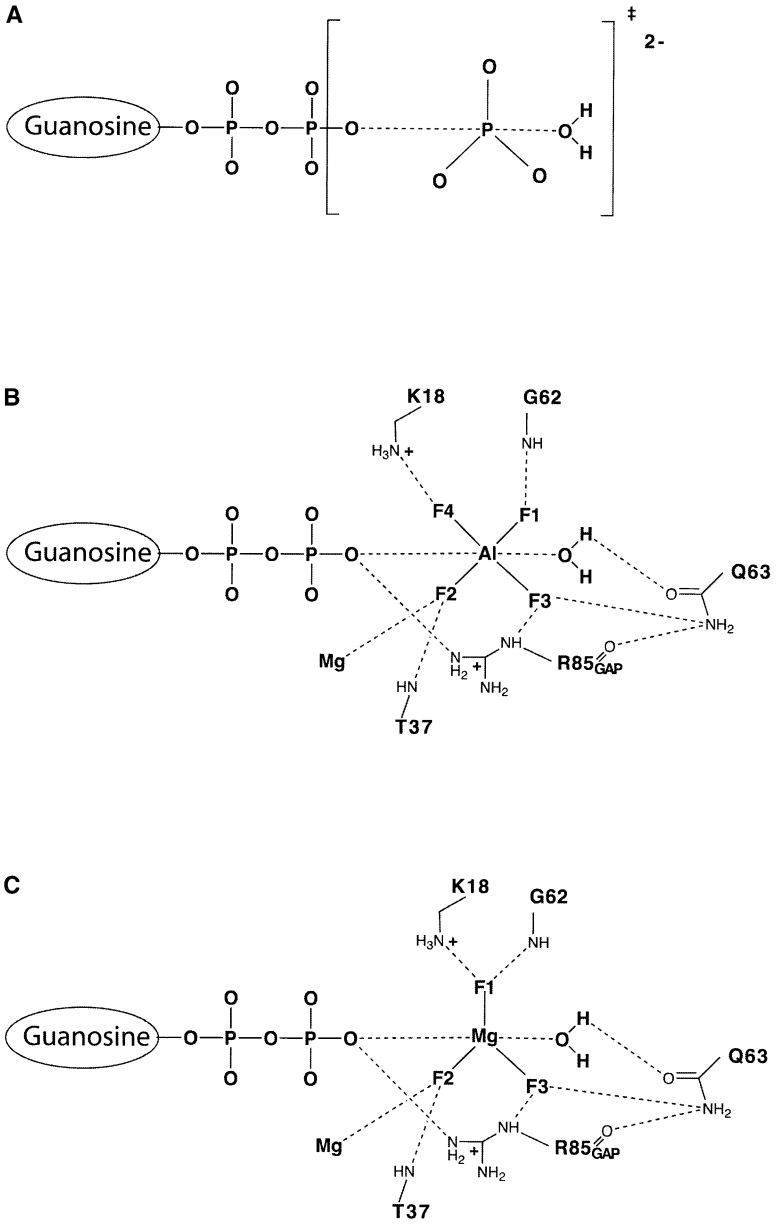

Figure 2. Schematic Diagrams of the Transition State of Phosphoryl Transfer Reaction

(A) shows a schematic representation of the transition state for a phosphoryl transfer reaction involving a trigonal bipyramidal phosphoryl group. There is controversy as to the degree of the associative or dissociative nature of the transition state and so the distribution of the two negative charges over the equatorial and axial oxygens coordinated to the γ-phosphorus is uncertain. A reaction mechanism which is dissociative will lead to an increase in the negative charge on the β-γ bridge oxygen upon transition state formation while an associative mechanism will increase the negative charge on the phosphoryl group being transferred. The conformation adopted by the catalytic arginine residue from RhoGAP is such that it could provide transition state stabilization for either type of reaction mechanism as is shown in (B) and (C). (B) and (C) show schematically the structures of the transition states analogs GDP.AlF_4^-.H_2O and GDP.MgF_3^-.H_2O, respectively, together with their interactions with the hydrolytic water, the nucleotide-associated magnesium, and residues K18, G62, Q63, and T37 from the G protein and R85 from RhoGAP.

responsible for BeF_3^-, in complex with NDP's, being regarded as a mimic of the ground state or Michaelis complex of many phosphoryl transfer enzymes. For example, the binding of BeF_3^- to Ras.GDP leads to the small G protein adopting an active, GTP bound-like conformation [24]. In contrast, small G proteins do not bind to either aluminum or magnesium fluorides in the absence of their cognate GTPase-activating protein.

Although there is still some controversy as to whether the hydrolysis of GTP by GTPases proceeds by an associative, dissociative, or mixed mechanism, it is clear that the expected transition state will involve the γ-phosphate group adopting a trigonal bipyramidal arrangement with the hydrolytic water molecule (Figure 2A). A similar arrangement is adopted by AlF_3 in various crystal structures involving GTPases and kinases. However, this aluminum fluoride species does not carry a net charge. In contrast, AlF_4^- does carry a net negative charge which would better approximate the expected charge for the transition state of a phosphoryl transfer reaction, but it adopts a square pyramidal geometry. That both AlFx species are found in crystal structures of GTPases means that the active sites of these enzymes are able to accommodate either species without much energetic cost. Our structural data establish that the magnesium fluoride species which binds to the active site of GTPases is MgF_3^-. This species has both the geometry and charge characteristics expected for the transition state of a phosphoryl transfer reaction.

The structural and spectroscopic data presented here rationalize and extend the utility of metallo-fluorides as transition state mimics for phosphoryl-transferring enzymes. Schlichting and Reinstein [25] have directly demonstrated that the pH of the crystallization experiment

Table 2. PIXE Analysis of Crystals

Metal Content (ppm)		Mg	Al	P
"MgF_3" crystal	1	880	<23*	1140
Measurement number	2	696	<22*	1082
	3	657	<20*	998
	4	643	<20*	929
	5	672	<25*	1195
"AlF_4" crystal	1	341	348	900
Measurement number	2	439	456	1278
	3	469	445	1236
	4	411	483	1378
	5	364	558	1165
Ratio of Metal Contents for	Mg:P	Al:P	Mg:Al	
MgF_3	0.86 (0.1)			
AlF_4	0.34 (0.04)	0.39 (0.05)	0.9 (0.16)	

*indicates measurement is below the minimum detectable level
Values in parentheses are standard deviations based on the five measurements.

determines whether AlF_3 or AlF_4^- is present at the active site of UMP/CMP kinase and, by analogy, in other phosphoryl-transferring systems. Their survey of all available crystal structures containing AlF_x concluded that structures determined at and below pH 7.0 contain AlF_4^-, while those crystallized above pH 7.0 contain AlF_3. Only one high-resolution structure (better than 2.5 Å) does not obey this trend. The structure of Cdc42/Cdc42GAP [9] (Cdc42GAP is identical to p50RhoGAP) was reported to contain AlF_3 despite being crystallized at pH 6.0. However, the crystallization conditions used in this case contained 200 mM Mg^{2+} and 0.1 mM Al^{3+}. Thus, in the light of the data presented here, it is possible to speculate that these crystals actually contained MgF_3^- bound at the active site of the G protein.

Data have been presented recently suggesting that the affinity of RhoGAP for Rho.GDP is approximately the same in the presence of magnesium or aluminum fluoride [17]. However, these data cannot be interpreted simply in terms of the two compounds having similar affinities for the active site of the Rho.GDP/RhoGAP complex. The concentrations of the relevant species in solution, together with any entropic differences upon binding of the two moieties, would make their apparent binding constants an unreliable indicator of their complementarity to the enzyme's active site. From the structural data presented here, together with our current understanding of phosphoryl transfer reactions, it seems that MgF_3^- has both the geometry and charge characteristics consistent with the phosphoryl transfer event whereas AlF_x species do not. This in turn suggests that magnesium fluoride may prove to be a superior reagent for future structural and kinetic studies involving phosphoryl transfer reactions.

Significance

Transition state analogs are widely used in enzymology as kinetic and structural tools. The study of phosphoryl transfer reactions in biological systems has been greatly facilitated by the use of alumino-fluorides as transition state mimics. These compounds, located at the active site of GTPases or kinases, are coordinated by oxygen atoms from the β-phosphate group of the nucleotide on one side, and the hydrolytic water molecule on the other. Two different alumino-fluoride

Table 3. Summary of Interaction Distances at the Active Site of RhoA/RhoGAP Complexes with AlF_4^- and MgF_3^-

Interacting Pairs	Distance Å	
	AlF_4^-	MgF_3^-
Metal—hydrolytic water (W1)	1.87	2.28
Metal—O3B phosphate	1.92	2.02
Rho Gln63 NE2—F3	2.93	2.92
Rho Gln63 OE1—hydrolytic water (W1)	2.68	2.58
Rho Thr37 OG1—nucleotide-associated Mg	3.15	2.22
(AlF_4^-) F4—nucleotide-associated Mg	2.61	—
(MgF_3^-) F2—nucleotide-associated Mg	—	2.28
Rho Thr37 main chain carbonyl—hydrolytic water (W1)	2.89	2.88
Rho Thr37 main chain NH—(Alf_4^-) F2	2.64	—
Rho Thr37 main chain NH—(MgF_3^-) F2	—	2.93
GAP Arg85 main chain carbonyl—Rho Gln63 NE2	2.87	2.90
GAP Arg85 NE—F3	2.73	2.89
GAP Arg85 NH2—O3B	3.11	2.91
Rho Lys 18 NZ—F4(AlF_4^-)	2.72	—
Rho Lys 18 NZ—F1(MgF_3^-)	—	2.77
Rho Gly N—F1(AlF_4^-)	2.88	—
Rho Gly N—F1(MgF_3^-)	—	2.88

species, AlF_3 and AlF_4^-, have been observed in crystal structures. Crystallization below pH 7.0 seems to favor AlF_4^- while higher pH results in binding of AlF_3. AlF_3 adopts a trigonal planar arrangement at the active site but carries no net charge. In contrast, AlF_4^- is square planar and carries a net negative charge. Although AlF_3 has the geometry expected for the transition state of a phosphoryl transfer reaction, AlF_4^- has a more appropriate charge. Nonetheless, both species appear to mimic the transition state to some extent. Recent biochemical data have suggested that magnesium fluoride may also be able to act as a transition state mimic of phosphoryl transfer reactions. We show here, by high-resolution X-ray crystallographic analysis of RhoA.GDP/RhoGAP, that trigonal planar MgF_3^- binds to the active site and coordinates oxygen atoms of the β-phosphate and hydrolytic water molecule in the axial positions. Given that this is an unusual coordination for magnesium, we have confirmed directly that the species present in the crystals is magnesium fluoride by proton-induced X-ray emission (PIXE) spectroscopy. The geometry and charge of this species are those suited to mimicking the trigonal bipyramidal phosphoryl transition state. Our data lead us to suggest that magnesium fluoride may be a reagent of choice for studying biological phosphoryl transfer reactions.

Experimental Procedures

RhoA and RhoGAP (fragment 198–439) were expressed as GST-fusion proteins and purified as previously described [13]. For crystallization, Rho.GDP and RhoGAP were mixed in a 1:1 molar ratio in the presence of 10 mM $MgCl_2$, 10 mM NaF, and 2 mM deferoxamine under otherwise similar conditions to those previously reported for the crystallization of the RhoGDP.AlF_4^-/RhoGAP complex [13]. Diffraction data were collected at ESRF and processed with the DENZO and SCALEPACK [26] software. Molecular replacement calculations were carried out with the Amore package using separate models for the RhoA and RhoGAP, both taken from 1TX4 on the Brookhaven Database. All subsequent calculations were carried out with the CCP4 program suite [27] and model-building was done using O [28].

The use of PIXE, especially with respect to the Oxford scanning proton microprobe facility, has recently been reviewed in some detail [20], [22]. Crystals were washed in de-ionized water, mounted on thin mylar films (1–2 μ), and manually dried prior to analysis. Single crystals, of both the AlF_4^- and MgF_3 types (approximate size 100 × 30 × 30 μm), were first scanned to obtain an image of the crystals before selecting 5 distinct sites for quantitative analysis. The experiment was carried out using a proton beam energy of 1.7 MeV in order to enhance the detection limits for Mg, Al, and P. Detection limits of 30–40 ppm were achieved for Mg at 1.7 MeV. The energy spectrum of recoiling protons was also recorded simultaneously with the PIXE spectrum for each point. This technique, known as Rutherford backscattering [21], allows the thickness and major element composition of the sample to be determined, together with the total beam charge. This additional information allows the PIXE spectra to be processed to obtain accurate elemental concentrations without routine reference to standards. The concentrations of magnesium, aluminum, and phosphorus in parts per million were extracted from the X-ray spectrum by the peak-fitting software GUPIX. The numbers of atoms present are calculated from the concentration measurements for each atom divided by their atomic mass.

Acknowledgments

We would like to thank G. Davies and J. Turkenburg for assistance with data collection, and G. Dodson, A. Lane, and D. Trentham for critical reading of this manuscript.

Received: July 19, 2001
Revised: December 14, 2001
Accepted: January 8, 2002

References

1. Sternweis, P.C., and Gilman, A.G. (1982). Aluminum: a requirement for activation of the regulatory component of adenylate cyclase by fluoride. Proc. Natl. Acad. Sci. USA *79*, 4888–4891.
2. Martin, R.B. (1988). Ternary hydroxide complexes in neutral solutions of Al3+ and F. Biochem. Biophys. Res. Commun. *155*, 1194–1200.
3. Martin, R.B. (1996). Ternary complexes of Al3+ and F- with a third ligand. Coordination Chemistry Reviews *141*, 23–32.
4. Bigay, J., Deterre, P., Pfister, C., and Chabre, M. (1985). Fluoroaluminates activate transducin-GDP by mimicking the gamma-phosphate of GTP in its binding site. FEBS Lett. *191*, 181–185.
5. Maegley, K.A. Admiraal, S.J., and Herschlag, D. (1996). Ras-catalyzed hydrolysis of GTP: A new perspective from model studies. Proc. Natl. Acad. Sci. USA *93*, 8160–8166.
6. Xu, Y.W., Morera, S., Janin, J., and Cherfils, J. (1997). AlF3 mimics the transition state of protein phosphorylation in the crystal structure of nucleoside diphosphate kinase and MgADP. Proc. Natl. Acad. Sci. USA *94*, 3579–3583.
7. Schlichting, I., and Reinstein, J. (1997). Structures of active conformations of UMP kinase from Dictyostelium discoideum suggest phosphoryl transfer is associative. Biochemistry *36*, 9290–9296.
8. Scheffzek, K., Ahmadian, M.R., Kabsch, W., Wiesmuller, L., Lautwein, A., Schmitz, F., and Wittinghofer, A. (1997). The Ras-RasGAP complex: structural basis for GTPase activation and its loss in oncogenic Ras mutants. Science *277*, 333–338.
9. Nassar, N., Hoffman, G.R., Manor, D., Clardy, J.C., and Cerione, R.A. (1998). Structures of Cdc42 bound to the active and catalytically compromised forms of Cdc42GAP. Nat. Struct. Biol. *5*, 1047–1052.
10. Sondek, J., Lambright, D.G., Noel, J.P., Hamm, H.E., and Sigler, P.B. (1994). GTPase mechanism of Gproteins from the 1.7-A crystal structure of transducin alpha-GDP-AIF-4. Nature *372*, 276–279.
11. Coleman, D.E., Berghuis, A.M., Lee, E., Linder, M.E., Gilman, A.G., and Sprang, S.R. (1994). Structures of active conformations of Gi alpha 1 and the mechanism of GTP hydrolysis. Science *265*, 1405–1412.
12. Fisher, A.J., Smith, C.A., Thoden, J.B., Smith, R., Sutoh, K., Holden, H.M., and Rayment, I. (1995). X-ray structures of the myosin motor domain of Dictyostelium discoideum complexed with MgADP.BeFx and MgADP.AlF4. Biochemistry *34*, 8960–8972.
13. Rittinger, K., Walker, P.A., Eccleston, J.F., Smerdon, S.J., and Gamblin, S.J. (1997). Structure at 1.65 A of RhoA and its GTPase-activating protein in complex with a transition-state analogue. Nature *389*, 758–762.
14. Higashijima, T., Ferguson, K.M., Sternweis, P.C., Ross, E.M., Smigel, M.D., and Gilman, A.G. (1987). The effect of activating ligands on the intrinsic fluorescence of guanine nucleotide-binding regulatory proteins. J. Biol. Chem. *262*, 752–756.
15. Antonny, B., Bigay, J., and Chabre, M. (1990). A novel magnesium-dependent mechanism for the activation of transducin by fluoride. FEBS Lett. *268*, 277–280.
16. Vincent, S., Brouns, M., Hart, M.J., and Settleman, J. (1998). Evidence for distinct mechanisms of transition state stabilization of GTPases by fluoride. Proc. Natl. Acad. Sci. USA *95*, 2210–2215.
17. Graham, D.L., Eccleston, J.F., Chung, C.W., and Lowe, P.N. (1999). Magnesium fluoride-dependent binding of small G proteins to their GTPase-activating proteins. Biochemistry *38*, 14981–14987.
18. Rittinger, K., Walker, P.A., Eccleston, J.F., Nurmahomed, K., Owen, D., Laue, E., Gamblin, S.J., and Smerdon, S.J. (1997). Crystal structure of a small G protein in complex with the GTPase-activating protein rhoGAP. Nature *388*, 693–697.
19. Evers, A., Hancock, R.D., Martell, A.E., and Motekaitis, R.J.

(1989). Metal-ion recognition in ligands with negatively charged oxygen donor groups - complexation of Fe(III), Ga(III), Al(III), and other highly charged metal-ions. Inorganic Chemistry *28*, 2189–2195.

20. Grime, G.W. (2001). High energy ion beam analysis (methods and background). In Encyclopedia of Spectroscopy, J. Lindon, G. Tranter, and J. Holmes, eds. (London: Academic Press).
21. Grime, G.W., Dawson, M., Marsh, M., McArthur, I.C., and Watt, F. (1991). The Oxford submicron nuclear microscopy facility. Nucleic Instr. Methods Phys. Res. *B 54*, 52–63.
22. Garman, E. (1999). Leaving no element of doubt: analysis of proteins using microPIXE. Structure Fold. Des. *7*, R291–R299.
23. Holloway, C.E., and Melnik, M. (1994). Magnesium compounds - classification and analysis of crystallographic and structural data. Journal of Organometallic Chemistry *465*, 1–63.
24. Diaz, J.F., Sillen, A., and Engelborghs, Y. (1997). Equilibrium and kinetic study of the conformational transition toward the active state of p21(Ha-ras), induced by the binding of BeF3- to the GDP-bound state, in the absence of GTPase-activating proteins. J. Biol. Chem. *272*, 23138–23143.
25. Schlichting, I., and Reinstein, J. (1999). pH influences fluoride coordination number of the AlFx phosphoryl transfer transition state analog. Nat. Struct. Biol. *6*, 721–723.
26. Otwinowski, Z., and Minor, W. (1997). Processing of X-ray diffraction data collected in oscillation mode. Methods Enzymol. *276*, 307–326.
27. CCP4. (1994). The CCP4 (Collaborative Computational Project Number 4) suite: programs for protein crystallography. Acta Crystallogr. D *50*, 307–326.
28. Jones, T.A., Zou, J.Y., and Cowan, S.W. and Kjeldgaard (1991). Improved methods for binding protein models in electron density maps and the location of errors in these models. Acta Crystallogr. A *47*, 110–119.
29. Carson, M. (1991). Ribbons 2.0. J. Appl. Crystallogr. *24*, 958–961.